

## Performance Evaluation of Modelling and Simulation of Lead Acid Batteries for Photovoltaic Applications

A. Selmani\*, A. Ed-Dahhak\*\*, M. Outanoute\*, A. Lachhab\*\*, M. Guerbaoui\* and B. Bouchikhi\*

\* Sensors Electronic & Instrumentation Team, Department of Physics, Faculty of Sciences,  
Moulay Ismaïl University, Meknes, Morocco

\*\* Modelling Systems Control and Telecommunications Team, High School of Technology,  
Moulay Ismaïl University, Meknes, Morocco

---

### Article Info

#### Article history:

Received Sep 22, 2015

Revised Feb 4, 2016

Accepted Feb 23, 2016

---

#### Keyword:

Battery charger

CIEMAT

LabVIEW/Multisim

Lead acid batteries

Modelling

Photovoltaic

---

### ABSTRACT

Lead-acid batteries have been the most widely used energy storage units in stand-alone photovoltaic (PV) applications. To make a full use of those batteries and to improve their lifecycle, high performance charger is often required. The implementation of an advanced charger needs accurate information on the batteries internal parameters. In this work, we selected CIEMAT model because of its good performance to deal with the widest range of lead acid batteries. The performance evaluation of this model is based on the co-simulation LabVIEW/Multisim. With the intention of determining the impact of the charging process on batteries, the behaviour of different internal parameters of the batteries was simulated. During the charging mode, the value of the current must decrease when the batteries' state of charge is close to be fully charged.

Copyright © 2016 Institute of Advanced Engineering and Science.  
All rights reserved.

---

### Corresponding Author:

Benachir Bouchikhi,

Sensors Electronic & Instrumentation Team, Department of Physics,

Faculty of Sciences Meknes, Moulay Ismaïl University

B.P. 11201, Zitoune, 50003, Meknes, Maroc,

E-mail: benachir.bouchikhi@gmail.com

---

## 1. INTRODUCTION

Batteries are influential component in stand-alone PV systems so they are the origin of the failure and loss of dependability. They guarantee an uninterrupted power supply to the load and compensate the power production deficiency whenever weather conditions are critical. To reduce the quantity of physical testing with a specific application, an accurate system modelling of batteries is required for an appropriate analysis and simulation. But modelling and estimation of batteries state of charge are known as one of the most complex tasks. Most of models necessitate the knowledge of proper parameters whose values have to be built-in for each specific battery design and capacity. This requires a complete testing process that is often beyond the usual datasheet of the constructor which is at once pricey and time consuming. Therefore, batteries behaviour has been basically labelled by many authors, and several mathematical models have been defined [1]–[4]. To avoid those mathematical descriptions while evaluating batteries output voltage, a new fuzzy based model for Nickel Cadmium (Ni-Cd) batteries was proposed [5]. Also, the extended Kalman filter is able to keep an exceptional precision in SOC estimation of Lithium-ion batteries [6]. However, the advantage of the battery models elaborated by Monegon and CIEMAT is underlined under their ability to cope with the widest range of lead acid batteries and requires few manufacture parameters [7]–[11]. The validity of such models was analysed in term of their capability to represent voltage evolution of batteries during charge and discharge processes. As a result, CIEMAT model proofs a good representation compared to Monegon model [12]. So, we chose the former model as an equivalent circuit structure for lead-acid

batteries simulation. This model and its implementation which is based on the co-simulation LabVIEW/Multisim are described in detail. This co-simulation is able to provide accurate simulation results and a very fast simulation speed. Thereby, it reveals the strong instantaneous relationship between the internal batteries parameters and the charging current rate.

## 2. BATTERY MODEL

### 2.1. Equivalent Circuit

Our study is founded on the model that was established by “Centro de Investigaciones Energéticas, Medioambientales y Tecnológicas” (CIEMAT) and based on the circuit shown in Figure 1. This equivalent circuit is composed of a voltage source  $V_1$  in series with internal resistance  $R_1$  which their characteristics depends on some parameters such as internal temperature ( $T$ ) and  $SOC$ .

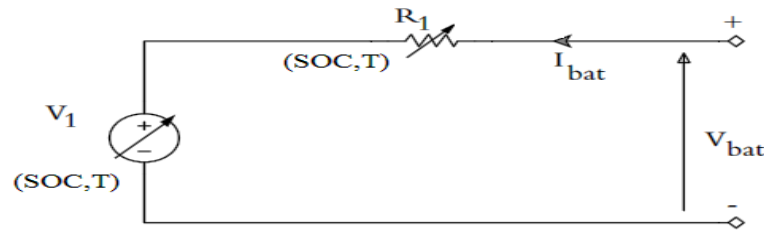


Figure 1. Battery model equivalent circuit

The implementation of the model of  $n_s$  cells in series implies necessarily assigning dissimilar expressions to the values of  $V_1$  and  $R_1$  in each different mode. We limit our study to the two main modes of operation: charge and discharge. For this reason, mathematical formulations are given by the following equations:

#### Charging mode

The electromotive force  $V_1$  and the internal resistor  $R_1$  are functions of the internal components of the battery:

$$\begin{aligned} V_1 &= n_s (2 - 0.16 SOC) \\ R_1 &= n_s \frac{I_{bat}}{C_{10}} \left( \frac{6}{1 + I_{bat}^{0.86}} + \frac{0.48}{(1 - SOC)^{1.2}} + 0.036 \right) (1 - 0.025 \Delta T) \\ V_{bat} &= V_1 + R_1 I_{bat} \end{aligned} \quad (1)$$

Where  $n_s$  is the cells number,  $\Delta T$  is the variation of the battery internal temperature ( $T_{bat}$ ),  $SOC$  is the battery state of charge at a given time,  $I_{bat}$  is the instantaneous battery current,  $V_{bat}$  is the instantaneous battery voltage, and  $C_{10}$  is the rated capacity.

#### Discharging mode

The mathematical equations are analogous to those found at charging mode with a sort of difference concerning the values.

$$\begin{aligned} V_1 &= n_s [2.085 - 0.12 (1 - SOC)] \\ R_1 &= n_s \frac{I_{bat}}{C_{10}} \left( \frac{4}{1 + I_{bat}^{1.3}} + \frac{0.27}{SOC^{1.5}} + 0.02 \right) (1 - 0.007 \Delta T) \\ V_{bat} &= V_1 - R_1 I_{bat} \end{aligned} \quad (2)$$

### 2.2. Capacitor Model

The capacity model is defined by the following equation (3). The value of the internal capacity ( $C_{bat}$ ) is settled from the expression of the current  $I_{10}$ , which match up to the operating speed of the rated capacity of the battery  $C_{10}$ .

$$\frac{C_{bat}}{C_{10}} = \frac{1.67}{1 + 0.67 \left(\frac{I_{bat}}{I_{10}}\right)^{0.9}} (1 + 0.005 (T_{bat} - 25)) \tag{3}$$

The instantaneous calculated capacity  $C_{bat}$  is used to estimate the *SOC* [13], as demonstrated in the equations below:

$$SOC(t) = SOC(t-1) + \frac{I_{bat}}{C_{bat}} \tag{4}$$

$$0 \leq SOC(t) \leq 1$$

**2.3. Thermal Model**

Equation (5) evaluates the change in electrolyte temperature, due to the internal resistive losses and the ambient temperature [9], [14]. The thermal model is defined by a first order differential equation with parameters for thermal resistance and capacitance. This has been done by the following equation:

$$T_{bat}(t) = T_0 + \frac{1}{C_o} \int_0^t \left( P_s - \frac{T_{bat}(\tau-1) - T_a}{R_o} \right) d\tau \tag{5}$$

Where  $T_{bat}$  is the battery’s temperature in °C;  $T_0$  is the battery’s initial temperature in °C, expected to be equal to the nearby ambient temperature;  $P_s$  is the  $R_l I_{bat}^2$  power loss of the internal resistance  $R_l$  in Watts;  $R_o$  is the thermal resistance in °C/Watts;  $C_o$  is the thermal capacitance in Joules/°C;  $\tau$  is an integration time variable; and  $t$  is the simulation time in seconds.

Even though the battery module is composed of more than one element, a single temperature for the electrolyte of the complete module was adopted.

**3. BATTERY MODEL SIMULATION STRUCTURE**

The National Instruments Community presents the principle of co-simulation using the two simulators LabVIEW and Multisim [15]. Therefore, the battery modelling and simulation are developed in the following manner. Firstly, the stage circuitry is designed in Multisim which contains three parts: an equivalent circuit model, a charge or discharge mode switcher, and a thermal model. Then the LabVIEW code to monitor the circuit is developed, located inside of a LabVIEW control bloc, and coupled to the Multisim circuit for co-simulation. The two simulators usually exchange data in a synchronised and variable time step manner. The flowchart of the proposed LabVIEW/Multisim battery model simulation is shown in the Figure 2.

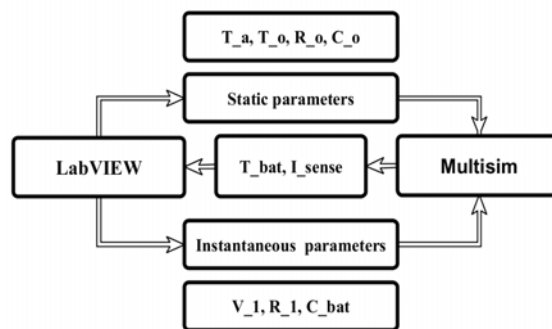


Figure 2. Flowchart of the proposed LabVIEW/Multisim battery model simulation

LabVIEW code sends two different types of data to Multisim circuitry. The first type is the static parameters used to define the thermal model, such as the ambient temperature ( $T_a$ ), the initial temperature ( $T_o$ ), the thermal resistance ( $R_o$ ) and the thermal capacitance ( $C_o$ ). The second type is the instantaneous parameters which evaluate the battery circuit parameters such as the voltage source ( $V_1$ ), the internal

resistance ( $R_I$ ) and the internal capacitance ( $C_{bat}$ ). On the other side, the calculation of those parameters within LabVIEW code depends on the data sent by Multisim stage such as the instantaneous battery temperature ( $T_{bat}$ ) evaluated by the thermal model bloc and the sensed current ( $I_{sense}$ ) through the equivalent circuit.

### 3.1. Multisim Stage

The equivalent circuit in Figure 3-a is composed of a voltage controlled source  $V_I$  in series with a voltage controlled resistor  $R_I$ . The values of  $V_I$  and  $R_I$  depend on the battery operation mode at a given time and varied with temperature and SOC. The resistance also varied with the sensed current ( $I_{sense}$ ) flowing through the current probe  $XCPI$ .

The charge and discharge mode switcher  $K_I$  is shown in Figure 3-b. It offers the possibility to switch between two modes according to the sent value by mean of the terminal  $Sw\_I$ . At charging time ( $Sw\_I = 5$  V) the positive battery pin (2) is linked to the controlled current source ( $I_{charge}$ ). But at discharging time ( $Sw\_I = 0$  V) the connection is switched to the voltage controlled resistor ( $R2$ ) instead.

The thermal Model in Figure 3-c trails the battery's electrolyte temperature. It is composed of two voltage controlled sources  $eq1$  and  $eq2$  which evaluate the instantaneous battery temperature ( $T_{bat}$ ). L. Castaner and S. Silvestre present the use of 'sdt' PSpice function which is the time integral operation [16]. We use this function to solve the equation (5) as the following:

- Voltage controlled source  $eq1$ :

$$\left( V(R_{bat}) * pwr(abs(V(I_{sense})), 2) \right) - (V(T_{bat}) - V(T_a)) / V(R_o) \tag{6}$$

- Voltage controlled source  $eq2$ :

$$V(T_o) + sdt(V(20)) / V(C_o) \tag{7}$$

The calculation of battery temperature  $V(T_{bat})$  is based on the internal resistance  $V(R_{bat})$  and the instantaneous sensed current through the battery  $V(I_{sense})$ . Moreover, the values of the ambient temperature  $V(T_a)$ , the thermal resistance  $V(R_o)$ , the battery initial temperature  $V(T_o)$  and the thermal capacitance  $V(C_o)$  are set at the beginning of the simulation and sent to Multisim by LabVIEW- Multisim terminals such as  $T_a$ ,  $R_o$ ,  $T_o$  and  $C_o$ . Finally the evaluated temperature  $V(T_{bat})$  is sent to LabVIEW code by the  $T_{bat}$  terminal.

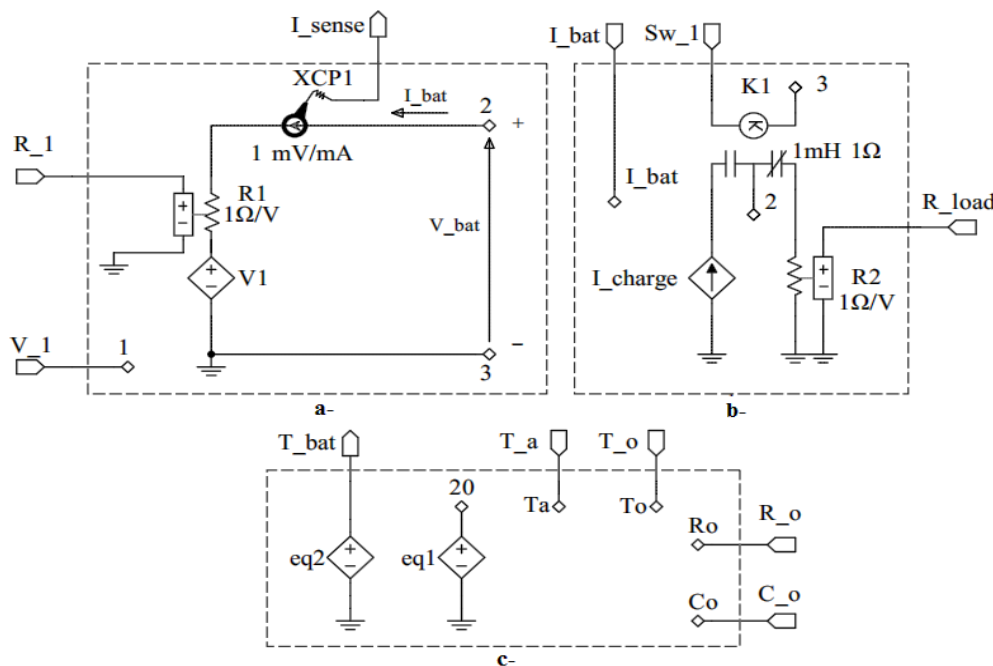


Figure 3. a- Equivalent circuit model, b- Charge or discharge mode switcher, c- Thermal model

**3.2. LabVIEW Stage**

Equations (1-4) which describe the evolution of internal battery parameters and the state of charge are implemented as separate collaborating blocks as shown in Figure 4. Therefore, the LabVIEW block diagram to control the Multisim battery circuitry contains three major parts: “Multisim Battery circuitry”, “Battery model parameters estimations” and “SOC estimation” block. The last two blocs execute the control system algorithms which estimate the battery model parameters. After that, the estimated values are sent to the Multisim circuit.

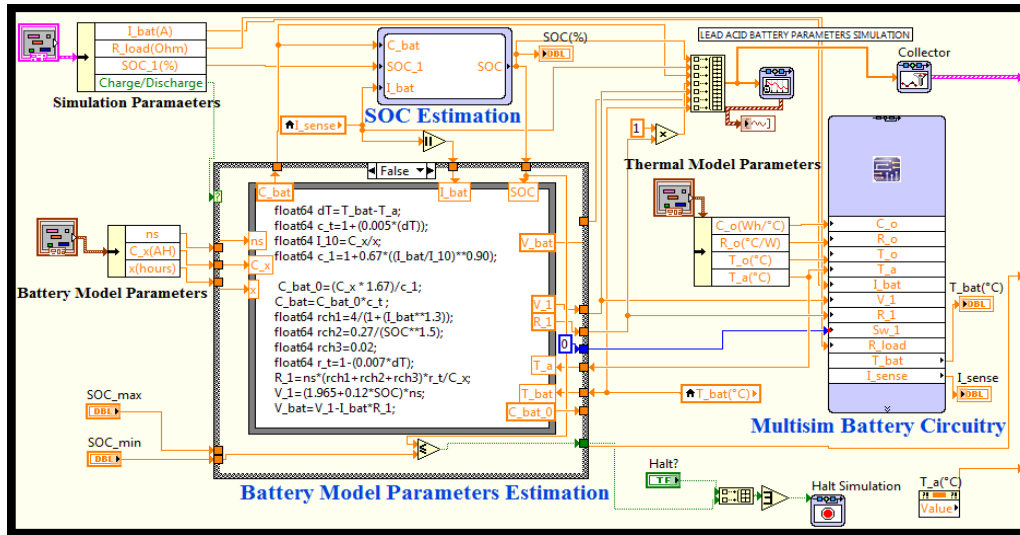


Figure 4. LabVIEW block diagram of battery model parameters estimation

**3.2.1. Battery Model Parameters Estimation Bloc**

The “Battery model parameters estimation” bloc is a LabVIEW case structure. It estimates, for every operation mode (charge or discharge), the instantaneous value of model parameters which are capacitance  $C_{bat}$  by using equations (1) and (2), internal voltage ( $V_1$ ) and internal resistor ( $R_1$ ) by using equations (3) and (4).

**3.2.2. SOC estimation bloc**

After the estimation of the internal parameters, the “SOC Estimation” bloc is then able to estimate the new instantaneous value of SOC by using the equation (4), as described in Figure 5. Hence, the calculation of SOC is based on the battery current ( $I_{bat}$ ), the estimated capacity ( $C_{bat}$ ) and the SOC history that is stored by the “Memory” block. The output of this memory bloc is limited between 0 and 1 by the “Saturation” bloc which presents the instantaneous estimated value of SOC.

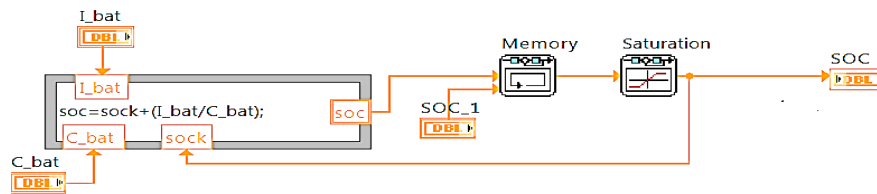


Figure 2. Battery state of charge estimation block

**4. RESULTS AND DISCUSSIONS**

**4.1. Simulation Results**

Figure 6 represents the front panel of the proposed LabVIEW graphical user interface (GUI) to simulate the instantaneous battery model parameters evolution. During the charging and discharging mode, it guaranties the observation of the behaviour of those internal parameters with the possibility of setting the

batteries datasheet parameters values manually. Additionally, we can test the impact of the current rate on batteries charging or discharging process: During the charging mode the GUI gives the possibility to define directly the value of the current, but during the discharging mode, this value is defined by varying the load resistance value. Moreover, the behaviour of each battery can be simulated at any given internal parameters' initial conditions, such as the internal temperature and the state of charge. In the next lines, the simulation results obtained during the charging mode will be presented. Firstly, we set battery models parameters (*battery 1*) as follow:

- Battery Model Parameters:  $n_s = 6$  and  $C_{10} = 190$  Ah;
  - Thermal Model Parameters:  $C_o = 15$  Wh/°C,  $R_o = 0.2$  °C/W,  $T_o = 25$  °C and  $T_a = 25$  °C.
- After that we set the simulation parameters by choosing the battery function mode (Charge) and setting the initial battery state of charge ( $SOC_I = 0.1$ ). Finally, we fix the charging current ( $I_{bat} = 1$  A).

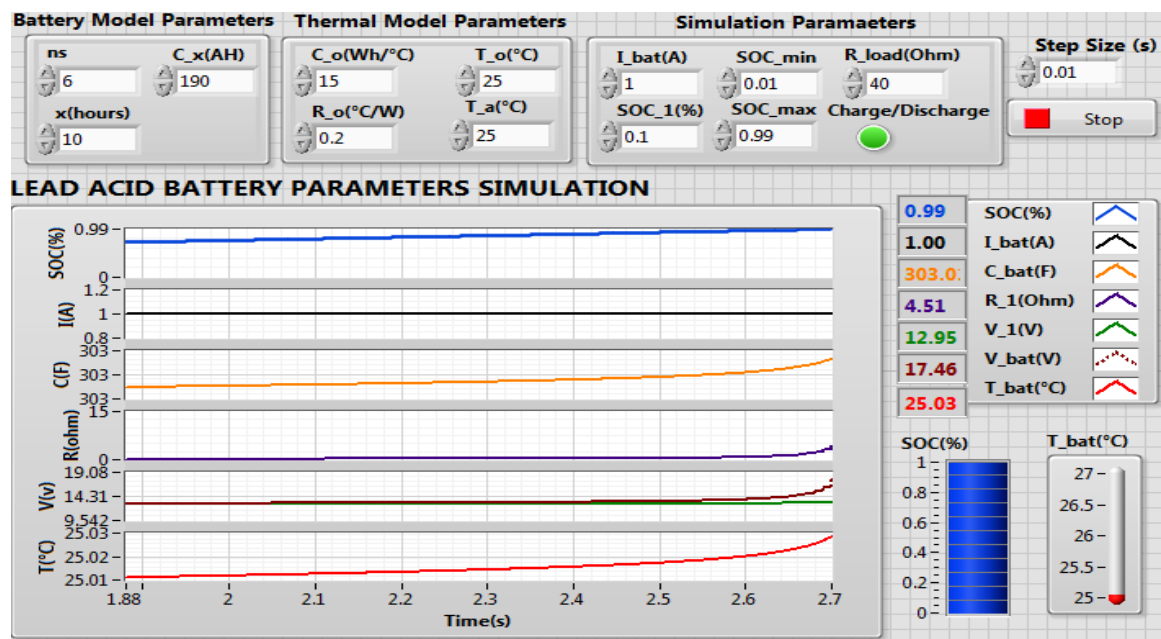


Figure 3. Lead acid battery parameters simulation GUI under co-simulation LabVIEW/Multisim

## 4.2. Discussions

To evaluate the performance of the proposed method of the modelling and simulation of lead acid batteries, a second battery (*battery 2*) is being simulated with the same thermal parameters and simulation conditions. The battery model parameters are:  $n_s = 6$ ,  $C_{10} = 296$  Ah.

Figure 7-a shows the evolution of internal resistance for the two batteries during the charging regime. The continuous curve refers to *battery 1*. Its internal resistance jumps from  $0.32 \Omega$  ( $SOC = 0.9$ ) to  $4.53 \Omega$  ( $SOC = 0.99$ ). The dashed curve refers to *battery 2*. Its internal resistance jumps from  $0.22 \Omega$  ( $SOC = 0.9$ ) to  $2.91 \Omega$  ( $SOC = 0.99$ ). As a result, when batteries are charging, the values of internal resistance are influenced by the state of charge. Moreover, those values increase rapidly when the batteries approach the fully charged state.

Figure 7-b shows the evolution of the variation of internal temperature for *battery 2* at three charging current rates. The amount of this variation is governed by both the charging current and the state of charge. During constant charging current, the temperature variation increases following the SOC. But, when we approach the fully charged state, the internal temperature value rises quickly with increasing charging current. Furthermore, the internal temperature influences the internal capacity. As a result, the capacity value of the battery becomes higher when it is close to be fully charged. This is why batteries require a long period of time in order to be fully charged.

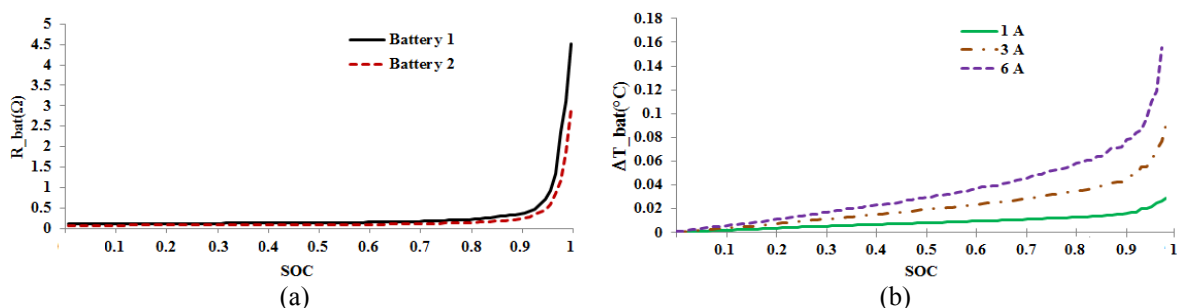


Figure 7. Evolution of internal parameters at charging time, a- Internal resistance, b- Internal temperature.

Traditional charging techniques of lead acid batteries either use constant current or constant voltage to charge batteries, or combine these two schemes. Constant current is practical at the beginning of battery charging while the battery voltage is low. When the battery voltage increases to a predefined value, the charger shifts to the constant voltage mode. However, when upcoming the fully charged state, the value of internal resistance increase rapidly which causes an exponential drop of the current. Therefore, full charge takes a long times which leads to very important change on the battery temperature. This fact has an important influence on the performance and lifetime of the batteries. To overcome those shortcomings, we intend to improve the performance of the charging process by an intelligent charging algorithm which can accurately determine that the charging current is necessary. A fuzzy logic system has been implemented to control the flow of charging current of Lithium-ion battery [17]. This controller will use two inputs which are voltage and temperature. The new charger will be based also on the fuzzy controller which takes into account the battery temperature variations and the SOC value when adjusting the charging current.

## 5. CONCLUSION

In this work we present a new method of simulation of lead acid batteries parameters. The implementation of the CIEMAT model was based on the co-simulation LabVIEW-Multisim. The circuitry stage is designed in Multisim and the code of controlling of this circuitry is developed in LabVIEW. The two simulators characteristically exchange data in a synchronized and variable time step mode. Simulation results demonstrate the impact of the charging current on the internal resistance, temperature and the capacitance of the battery. At charging time, internal resistance and temperature increase rapidly when approaching the fully charged state. Therefore, to improve the performance of the battery charging process by enhancing the full charge time, the battery charger control algorithm must take the internal temperature and the SOC information into account when evaluating the charging current. As a result, the charging current must drop when internal temperature or SOC rises. In the future work, we intend to implement a fuzzy-control-based battery charger to cop traditional charger fails. This control is taking the variation of temperature and SOC as input to adjust the charging current as an output.

## REFERENCES

- [1] M. Chen and G. A. Rincon-Mora, "Accurate Electrical Battery Model Capable of Predicting Runtime and I-V Performance", *IEEE Transactions on Energy Conversion*, vol. 21, no. 2, pp. 504–511, Jun. 2006.
- [2] F. M. González-Longatt, "Circuit Based Battery Models: A Review", in *Proceedings of 2nd Congreso Iberoamericano De Estudiantes de Ingeniería Electrica, Puerto la Cruz, Venezuela*, 2006.
- [3] O. Tremblay and L.-A. Dessaint, "Experimental Validation of a Battery Dynamic Model for EV Applications", *World Electric Vehicle Journal*, vol. 3, no. 1, pp. 1–10, 2009.
- [4] S. M. Mousavi G. and M. Nikdel, "Various Battery Models for Various Simulation Studies and Applications", *Renewable and Sustainable Energy Reviews*, vol. 32, pp. 477–485, Apr. 2014.
- [5] M. Sarvi and M. Safari, "A Fuzzy Model for Ni-Cd Batteries", *IAES International Journal of Artificial Intelligence (IJ-AI)*, vol. 2, no. 2, pp. 81–89, 2013.
- [6] F. Jin and H. Yong-ling, "State-Of-Charge Estimation of Li-ion Battery using Extended Kalman Filter", *TELKOMNIKA Indonesian Journal of Electrical Engineering*, vol. 11, no. 12, pp. 7707–7714, 2013.
- [7] J. B. Copetti, E. Lorenzo, and F. Chenlo, "A General Battery Model for PV System Simulation", *Progress in Photovoltaics: research and applications*, vol. 1, no. 4, pp. 283–292, 1993.
- [8] L. Castañer, R. Aloy, and D. Carles, "Photovoltaic System Simulation using a Standard Electronic Circuit Simulator", *Progress in Photovoltaics: Research and applications*, vol. 3, no. 4, pp. 239–252, 1995.

- [9] M. Ceraolo, "New dynamical Models of Lead-acid Batteries", *Power Systems, IEEE Transactions on*, vol. 15, no. 4, pp. 1184–1190, 2000.
- [10] S. Barsali and M. Ceraolo, "Dynamical Models of Lead-acid Batteries: Implementation Issues", *Energy Conversion, IEEE Transactions on*, vol. 17, no. 1, pp. 16–23, 2002.
- [11] O. Gergaud, G. Robin, B. Multon, and H. B. Ahmed, "Energy Modeling of a Lead-acid Battery within Hybrid Wind/Photovoltaic Systems", in *European Power Electronic Conference 2003*, 2003, pp. 1–8.
- [12] N. Achaibou, M. Haddadi, and A. Malek, "Modeling of Lead-acid Batteries in PV Systems", *Energy Procedia*, vol. 18, pp. 538–544, 2012.
- [13] S. Cho, H. Jeong, C. Han, S. Jin, J. H. Lim, and J. Oh, "State-of-Charge Estimation for Lithium-ion Batteries Under Various Operating Conditions using an Equivalent Circuit Model", *Computers & Chemical Engineering*, vol. 41, pp. 1–9, Jun. 2012.
- [14] R. A. Jackey, "A Simple, Effective Lead-acid Battery Modeling Process for Electrical System Component Selection", SAE Technical Paper, 2007.
- [15] "Community: Design Guide to Power Electronics Co-Simulation with Multisim and LabVIEW - National Instruments", 01-Nov-2011. [Online]. Available: <https://decibel.ni.com/content/docs/DOC-19212>.
- [16] L. Castaner and S. Silvestre, in *Modelling Photovoltaic Systems Using PSpice*, 1st ed., Chichester: Wiley, 2002, pp. 120–122.
- [17] R. Passarella, A. F. Oklilas, and T. Mathilda, "Lithium-ion Battery Charging System using Constant-Current Method with Fuzzy Logic Based ATmega16", *Int. J. Power Electron. Drive Syst. IJPEDS*, vol. 5, no. 2, pp. 166–175, 2014.

## BIOGRAPHIES OF AUTHORS



**A. Selmani** is a computer science teacher at qualifying school since 2001. Currently he is a Ph.D. student at the Electronics Automatic and Biotechnology Laboratory, Faculty of Sciences of Meknes, Moulay Ismail University, Morocco. His research interests include fuzzy logic controller based of the climate under greenhouse using solar energy equipment.



**A. Ed-dahhak** received Ph.D. from Faculty of Sciences Meknes in 2009. He is a Professor in the Department of Electrical Engineering, High School of Technology Meknes, Moulay Ismail University, Morocco. He is a member of Laboratory of Electronics, Automatics and Biotechnology of the Faculty of Sciences, Meknes. His current area of research includes electronics, development of a system for monitoring the climate and managing the drip fertilizing irrigation in greenhouse.



**M. Outanoute** is currently a Ph.D. student at the Electronics Automatic and Biotechnology Laboratory, Moulay Ismail University, Faculty of Sciences in Meknes, Morocco. His research interests include advanced modeling and control strategies of climatic parameters under a solar greenhouse.



**A. Lachhab** received Ph.D. from Faculty of Sciences in Rabat in 2000. He is a Professor in High School of Technology of Meknes, Moulay Ismail University, Morocco. He is a Member of Laboratory of Electronic, Automatic and Biotechnology in Faculty of Sciences in Meknes. His current area of research includes modelling and automatic control.



**M. Guerbaoui** received Ph.D. from Faculty of Sciences Meknes in 2014. He is a teacher at High School in Engineering Science since 1996. He is a member of Laboratory of Electronics, Automatics and Biotechnology of the Faculty of Sciences, Meknes. His research interests include regulating parameters under greenhouse by Fuzzy logic and use of solar energy equipment in the greenhouse.



**B. Bouchikhi** received the Ph.D. degree from the Université de droit, d'Economie et des Sciences d'Aix Marseille III, in 1982. Benachir Bouchikhi was awarded a Doctor of Sciences degree in 1988 from the University of Nancy I. Dr. Bouchikhi got a position of titular professor at the University of Moulay Ismaïl, Faculty of Sciences in Meknes, Morocco since 1993. He is the director of the Laboratory of Electronics, Automatic and Biotechnology. His current research focuses on the development of electronic nose and electronic tongue devices for food analysis and biomedical applications and the control of the climate and drip fertirrigation under greenhouse. He is author and co-author of over 65 papers, published on international journals. During the last 10 years he has coordinated a dozen national and international projects, in the area of food safety, the control of the climate and drip fertirrigation under greenhouse. He is member of the H2020-MSCA-RISE-2014 project TROPSENSE: "Development of a non-invasive breath test for early diagnosis of tropical diseases He is member of the Editorial Board of Journal of Biotechnology and Bioengineering.